ZnO-based visible-light photocatalyst: Band-gap engineering and multi-electron reduction by co-catalyst

Srinivasan Anandan[a], Naoki Ohashi[b], Masahiro Miyauchi[a],*

[a] National Institute of Advanced Industrial Science and Technology (AIST), Central 5, 1-1-1 Higashi, Tsukuba, Ibaraki 305-8565, Japan
[b] National Institute for Materials Science (NIMS), 1-1 Namiki, Tsukuba, Ibaraki 305-0044, Japan

ARTICLE INFO

ABSTRACT

Efficient ZnO based visible-light photocatalysts, Cu(II) modified $Cd_xZn_{1-x}O$ were developed by adopting a hybrid approach, consisting of band-engineering by formation of a solid solution and surface modification of co-catalysts. The $Cd_xZn_{1-x}O$ solid solution exhibited the visible-light activity for decomposing gaseous acetaldehyde, while bare ZnO showed negligible activity under visible-light. Further, the visible-light activity of $Cd_xZn_{1-x}O$ photocatalysts was greatly improved by the surface modification of Cu^{2+} ions. Photogenerated electrons in $Cd_xZn_{1-x}O$ are injected into the modified Cu^{2+} ions under visible-light irradiation, and electrons in Cu^{2+}/Cu^+ redox couples cause the efficient reduction of absorbed oxygen molecules. The strategy in the present study is a promising approach for applying ZnO-based photocatalysts for indoor applications.

© 2010 Elsevier B.V. All rights reserved.

1. Introduction

Since, indoor applications are in a high need of visible-light rather than UV light, the current research in photocatalysis is mainly focused on the fabrication of highly active visible-light driven photocatalyst. Doping of cations (transition metals) and anions (nitrogen, sulfur, carbon, or boron) into semiconductors have been extensively studied to enhance the activity of photocatalysts under visible-light irradiation. However, in spite of such extensive studies, most systems are still not satisfactory from the viewpoint of practical purposes. This is because, for example in the cation-doped semiconductors, the metal dopants introduced deep impurity levels in the forbidden band of the photocatalysts, which act as recombination centres, and thus impair the photocatalytic activity [1]. In case of anion-doped semiconductors, although nitrogen doped TiO_2 [2] is considered as one of the best candidates for visible-light driven photocatalysis, its quantum yield under visible-light is much less than that under UV light [3,4]. The localized N 2p level in this material was located above the valence band maximum (VBM). Thus, photogenerated holes produced by visible-light are localized with low oxidation power (2.25 V vs. SHE, pH 0 [5]) and have a slower mobility than those produced by a band-gap

excitation by UV illumination. Thus, it will be highly imperative to develop visible-light photocatalysts, in which the photo-produced holes in deep VB with high mobility and high oxidation power.

On the other hand, several groups recently reported a simple pristine metal oxide such as tungsten oxide (WO_3) as a visible-light-driven photocatalyst because of its small band-gap (2.8 eV) and a deeper VB (+3.1 V vs. SHE, pH 0 [6–9]). However, pure WO_3 was once considered to be photocatalytically inactive, owing to its low conduction band (CB) potential (0.3–0.5 V vs. SHE, pH 0 [6–9]), in which the photo-generated electrons cannot react with molecular oxygen through a one-electron reduction [10]. Recently, visible-light activity of WO_3 was greatly enhanced by the addition of co-catalysts, such as Pt [6], Cu^{2+} [7], Pd [8] or WC [9] via efficient oxygen reduction process. These co-catalysts act as electron pools to initiate multi-electron reductions (two-electron reduction: $O_2 + 2H^+ + 2e^- \rightarrow H_2O_2$, 0.68 V; or four-electron reduction: $O_2 + 2H_2O + 4H^+ + 4e^- \rightarrow 4H_2O$, 1.23 V) of the oxygen molecules to produce hydrogen peroxide molecules. It is noted that the quantum yield of WO_3 for decomposing gaseous iso-propanol is 17% [7], which is much higher than that of nitrogen doped TiO_2 [3]. These results indicate that a metal oxide with low conduction band like WO_3 becomes promising candidate for visible-light active photocatalysts, once its surface is modified by co-catalysts, which cause multi-electron reduction like Cu^{2+} ions. Even though the WO_3 is a good candidate for the efficient visible-light active photocatalyst, tungsten is rare metal with high cost and WO_3 is chemically unstable especially in alkaline solution, thus it is not appropriate for industrial use. Very recently, Yu et al. reported that the Ga and W co-doped TiO_2 with Cu^{2+} modification exhibited the visible-light

* Corresponding author. Tel.: +81 29 861 6299; fax: +81 29 861 6299.
E-mail address: m-miyauchi@aist.go.jp (M. Miyauchi).

activity, and its quantum yield under visible-light irradiation was 13% [11].

Considering these previous studies, we understood the following strategies are important to design an efficient visible-light active photocatalysts: (i) The dopants have the ability to absorb visible-light by CB control of semiconductors either forming the isolated state below the CB or to narrow the band-gap by shifting the CB bottom positively (ii) The VB of semiconductors must be in a deeper position upon band engineering and (iii) modification by co-catalysts onto the surface of photocatalyst to cause an efficient oxygen reduction similar like WO_3 [7]. These strategies encouraged us to fabricate a novel, low-cost and successful visible-light active photocatalyst alternative to TiO_2 and WO_3. In the present study, we have focused on the development of zinc oxide (ZnO)-based visible-light photocatalysts, which is in-expensive, easily available and seems to be an alternative to TiO_2 and WO_3. Zinc oxide is a direct wide gap semiconductor with a band-gap of 3.37 eV and found to be useful in various opto-electronic applications such as light emitting diodes, or solar cells, etc. [12–20]. Many efforts have been made to develop ZnO-based visible-light photocatalysts, particularly, combination with GaN [21] or Co doping [22] into ZnO were prepared to extend the absorption spectrum of ZnO into visible region.

In the present study, we used two processes to design visible-light active photocatalyst, i.e. (i) band engineering by a formation of ZnO based solid solution and (ii) multi-electron reduction by the modification of co-catalysts. Firstly, Cd^{2+} ions were incorporated into Zn sites to form the $Cd_xZn_{1-x}O$ solid solution for visible-light absorption. In fact, because of the similar structure of the electronic shell, transition metal cadmium has many physical and chemical properties similar to those of transition metal zinc. Since physical characteristics of Cd^{2+} are similar to Zn^{2+}, a substitution of Zn^{2+} by Cd^{2+} can result in the visible-light absorption without the formation of defects. Secondly, Cu^{2+} ions were modified onto the Cd^{2+}-incorporated ZnO to cause the multi-electron reduction. The visible-light photocatalytic activity of the resulting photocatalysts was evaluated by the decomposition of gaseous acetaldehyde under visible-light irradiation. Band structure of the resulting Cu(II) modified $Cd_xZn_{1-x}O$ photocatalysts was discussed based on the characterization and photocatalytic results.

2. Experimental details

2.1. Synthesis of cadmium zinc oxide ($Cd_xZn_{1-x}O$) solid solutions and Cu^{2+} modified $Cd_xZn_{1-x}O$

$Cd_xZn_{1-x}O$ photocatalyst was prepared by a hydrothermal process using cadmium acetate and zinc acetate as the source for Cd and Zn respectively. In a typical synthesis, 0.274 g of Zn $(CH_3COOH)_2 \cdot 2H_2O$ (Wako) and appropriate amount of $Cd(CH_3COOH)_2 \cdot 2H_2O$ (Wako) were dissolved in 60 mL of ethanol (99.5%, Wako) with stirring for 2 h. Further, 0.108 g of NaOH (Wako) was added to a resultant clear solution and stirred for another 1 h. The clear solution was then transferred to teflone lined autoclaves (100 mL capacity) and heated at 180 °C for 2 h. The samples were cooled, centrifuged and thoroughly washed with water until all the un-reacted compounds were removed. The samples were dried at 60 °C overnight to obtain $Cd_xZn_{1-x}O$, where x ranges from 0.05, 0.1, 0.15, 0.20 and 0.25. The Cu^{2+}-modified $Cd_xZn_{1-x}O$ photocatalyst was prepared by impregnation method [7] using $CuCl_2 \cdot 2H_2O$ (Wako) as the source for Cu(II). One gram of $Cd_xZn_{1-x}O$ was dispersed in 10 g of distilled water. $CuCl_2 \cdot 2H_2O$ was weighed so that the weight fraction of Cu relative to $Cd_xZn_{1-x}O$ was 1×10^{-3} (i.e., 1.57×10^{-5} mol of Cu). The weighed $CuCl_2 \cdot 2H_2O$ was then added to the aqueous suspension containing $Cd_xZn_{1-x}O$, heated at 90 °C for 1 h. The resulting suspension was filtered twice with water each 300 mL with a membrane filter (0.025 μm, Millipore) and dried at 60 °C for overnight. Finally the sample grinded using agate mortar to get fine powder of Cu^{2+}-modified $Cd_xZn_{1-x}O$ photocatalyst.

2.2. Characterization and evaluations

The crystal structures of ZnO, $Cd_xZn_{1-x}O$, and Cu^{2+}-modified $Cd_xZn_{1-x}O$ were analyzed by XRD with Cu Kα X-rays (Model: Ultima-x, Rigaku Ltd.). The grain size of the photocatalysts was calculated by Scherrer equation: $Dp = 0.9\lambda/(\beta_{1/2} \cos\theta)$ where Dp is the average grain size in Å, $\beta_{1/2}$ the full width of the peak at half maximum, and θ is the diffraction angle. The morphology of the $Cd_xZn_{1-x}O$ photocatalyst was observed by a transmission electron micorscopy (TEM; JEOL JEM-2100F, 200 kV). The specific surface area (BET) was estimated by the surface area apparatus (Belsorp-2, Bel Japan Ltd). The UV−vis absorption spectra of the photocatalysts were recorded with an UV−vis spectrophotometer (JASCO V-660) with an integration sphere using a reflection mode. For the direct band-gap semiconductor, the band-gap energy can be expressed by the following equation [23]: $(\alpha h\nu) = A (h\nu - E_g)^{1/2}$ where α is the absorption coefficient, $h\nu$ is the photon energy, A is constant, and E_g is the band-gap energy for direct transitions. The percentage of ionic character was calculated from the following equation: Percentage ionic character $= \{1 - (e^{-(X_A - X_B)^2})/4\} \times 100$ where X_A and X_B are the electro-negativity values of the elements involved in the bonding and the relevant values were obtained from standard sources. The electro-negativity values of Mg, Zn, Cd, and O are 1.3, 1.6, 1.7, and 3.4 respectively were used to calculate the percentage of ionic character. X-ray photoelectron spectroscopy (XPS) analysis was carried out with a Quantum 2000 microprobe system (Physical Electronics, Inc.) to analyze Zn/Cd ratio in the resultant photocatalyst. Photocatalytic oxidation activities of $Cd_xZn_{1-x}O$ powder were evaluated by gaseous acetaldehyde decomposition. For the photocatalytic measurements, 0.1 g of photocatalyst was uniformly dispersed on a circular glass dish, and the sample was pre-treated for 3 h using black light irradiation in air to clean the surface. The resulting sample was then mounted in a cylindrical glass air-filled static reactor (500 mL total volume) with quartz window. The O_2 (20%)–N_2 mixture adjusted to a relative humidity of 50% was used to fill the reaction vessel. Then, a certain amount of the gas-phase acetaldehyde was introduced into the reactor by syringe until the concentration reached about 500 ppmv. Before illumination, the catalyst and acetaldehyde were kept in the dark for 3 h to ensure the establishment of adsorption–desorption equilibrium between catalyst and acetaldehyde. The wavelength of visible-light ranged from 400 to 550 nm by using a blue–green LED. The intensity of visible-light, which was measured by a spectro-radiometer (USR-40D, Ushio Ltd), was 20 mW/cm^2. The concentration of acetaldehyde and the generation of CO_2 were measured using a gas chromatograph (Shimadzu, GC-8A) equipped with a 2 m Propak-Q column, a flame ionization detector, and a methanizer. In order to check the stability of $Cd_xZn_{1-x}O$ photocatalysts, 0.1 g of $Cd_xZn_{1-x}O$ photocatalyst was added into beaker containing 50 mL water which kept at neutral condition. The resulting mixture was stirred upto one week under dark as well as under visible-light illumination, and the samples were collected from the mixtures twice in a week (sample interval: one day and seven days). The collected samples were centrifuged, filtered by cellulose acetate syringe filter (Advantec, 0.2 μm). Then 0.5 mL of supernatant was taken and diluted to hundred times by adding required amount of water. The conentration of Cd and Zn in the above solution was analyzed by using high sensitive radiofrequency inductive coupled plasma (rf-ICP, Horiba Ultima2). The detection limit of rf-ICP instrument for Cd element is about 0.1 ppb. Cd (100 ppm, Wako) and Zn (100 ppm, Wako)
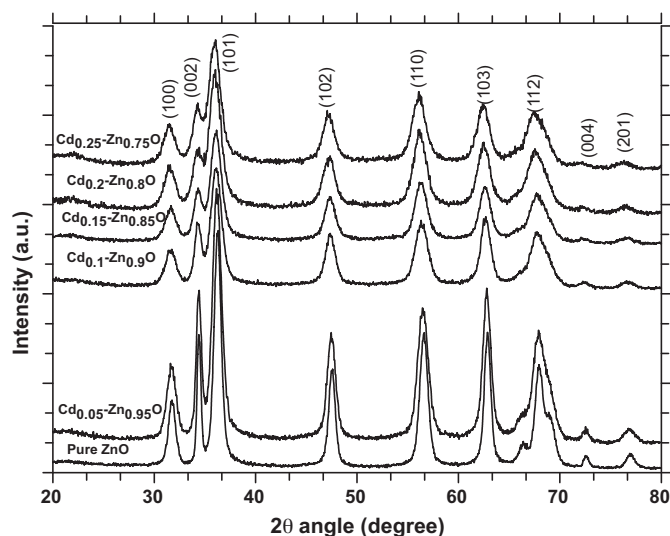
Fig. 1. X-ray diffraction patterns of pure ZnO and $Cd_xZn_{1-x}O$ photocatalysts.

standard solutions were used as standard and diluted to 1, 5 ppm solution for ICP analysis.

3. Results and discussion

3.1. X-ray diffraction and TEM studies

The XRD patterns of ZnO and $Cd_xZn_{1-x}O$ are shown in Fig. 1. The diffraction patterns of each sample were well in agreement with JCPDS card of ZnO (JCPDS 36-1451). These results indicate that the as-synthesized samples were single phase with a hexagonal wurtzite structure without a formation of impurities like CdO. Enlarged XRD patterns were shown in our supporting information (Fig. S1a), and the peak positions of wurtzite-type phase were shifted to lower angles with the increasing Cd concentration. The shifts in XRD patterns indicated that the crystals obtained were not the mixture of ZnO and CdO phases but $Cd_xZn_{1-x}O$ solid solutions. The shift of peaks to lower values was reasonable because the ionic radius of Cd^{2+} (0.078 nm) is larger than that of Zn^{2+} (0.060 nm) at tetrahedral site [24]. This shift also indicates the expansion of lattice by forming $Cd_xZn_{1-x}O$ solid solutions. Besides, as calculated from Debye–Scherrer equation, the average crystallite size of ZnO was 10.93 nm, while for $Cd_xZn_{1-x}O$ the size was in the range of 8–9 nm, implying the substitution of Cd^{2+} into Zn-site inhibits the grain growth. BET surface area of pure ZnO was about 63 m²/g. The surface area of $Cd_xZn_{1-x}O$ photocatalysts increased with the increasing concentration of Cd^{2+} as shown in Table 1, revealing that Cd^{2+} substitution increased the surface area of ZnO, which is consistent with the crystal size derived from XRD results. It should be also noted that XRD pattern of Cu^{2+}-modified $Cd_{0.1}Zn_{0.9}O$ (Fig. S1b) photocatalyst did not show any additional peaks other than wurtzite-type phase, indicating the presence of small amorphous CuO like clus-

ters, similar to the previous report [25]. These results conclude that Cu-modified $Cd_{0.1}Zn_{0.9}O$ photocatalysts retain the crystal structure similar to $Cd_{0.1}Zn_{0.9}O$, indicating that the Cu(II) modification does not influence changes in the crystal structure of $Cd_{0.1}Zn_{0.9}O$ photocatalysts. The crystal size derived from Debye–Scherrer equation was consistent with TEM images (Fig. 2), in which the mean diameter of the hexagonal particles was ∼9 nm. A selected area diffraction pattern (SAED) for the resulting $Cd_{0.1}Zn_{0.9}O$ (Fig. 2d) shows the (100), (101), (110), (002) and (003) reflections of ZnO, indicate that the $Cd_{0.1}Zn_{0.9}O$ photocatalysts are well crystallized.

3.2. X-ray photoelectron spectroscopic analysis

XPS measurement was used to determine the composition and the oxidation states of the synthesized samples and the results were shown in Table 2. The measured compositions of $Cd_xZn_{1-x}O$ powders by XPS analysis are deviated from the initial compositions in a hydrothermal solution as shown in Table 2. This is because of the variation in the solubility of Cd^{2+} or Zn^{2+} ions under hydrothermal conditions. However, the initial concentrations of Cd^{2+} and Zn^{2+} ions in solutions are used to describe the concentration of Cd^{2+} and Zn^{2+} ions throughout the manuscript. The amount of Cu(II) ions in Cu(II) modified $Cd_{0.1}Zn_{0.9}O$ photocatalysts with different concentration of Cu(II) measured by XPS analysis was less (0.03%, 0.08% and 0.25%) than compared to initial values (0.05%, 0.1% and 0.3%). XPS spectra of the as-synthesized $Cd_{0.1}Zn_{0.9}O$ photocatalysts are displayed in our supporting information (Fig. S2a–c), which exhibit the binding energy peaks of Zn $2p_{3/2}$ at 1021.9 eV; Zn $2p_{1/2}$ at 1045 eV, of O 1s at 530.5 eV, and of Cd $3d_{5/2}$ at 405.25; Cd $3d_{3/2}$ at 412.2 eV respectively. The binding energy peak values of Cd 3d and Zn 2p of $Cd_xZn_{1-x}O$ are in good agreement with the values reported previously [26,27], where the metal atoms present in Cd^{2+} and Zn^{2+} oxidation states respectively. Since there was no evidence for the formation of metallic Zn or metallic Cd [28], it is confirmed that Zn and Cd elements exist as Zn^{2+} and Cd^{2+} in $Cd_xZn_{1-x}O$. In addition, the shift of XRD peaks to lower values with the formation of very small crystal size (∼9 nm) of hexagonal particles in $Cd_xZn_{1-x}O$ solid solutions, reveals that Cd^{2+} may uniformly diffused into Zn^{2+} sites of ZnO crystals.

Table 2
Comparison of concentration of Cd^{2+} and Zn^{2+} ions measured by XPS analysis and experimental calculation.

Material	Concentration of elements			
	Experiment		XPS analysis	
	Zn	Cd	Zn	Cd
Pure ZnO	1.0	–	1.0	–
$Cd_{0.05}Zn_{0.95}O$	0.95	0.05	0.982	0.018
$Cd_{0.1}Zn_{0.9}O$	0.9	0.1	0.962	0.038
$Cd_{0.15}Zn_{0.85}O$	0.85	0.15	0.897	0.103
$Cd_{0.20}Zn_{0.80}O$	0.80	0.20	0.873	0.127
$Cd_{0.25}Zn_{0.75}O$	0.75	0.25	0.832	0.168

Table 1
Physico-chemical characteristics of pure ZnO and $Cd_xZn_{1-x}O$ photocatalysts.

Catalysts	Surface area (m²/g)	Crystal size[a] (nm)	Near band edge emission (nm)	Band-gap[b] (eV)
Pure ZnO	63.37	10.93	374	3.13
$Cd_{0.05}Zn_{0.95}O$	79.32	8.89	376	2.96
$Cd_{0.1}Zn_{0.9}O$	84.15	8.36	388	2.81
$Cd_{0.15}Zn_{0.85}O$	85.67	8.36	406	2.68
$Cd_{0.20}Zn_{0.80}O$	86.35	8.16	412	2.64
$Cd_{0.25}Zn_{0.75}O$	88.92	7.89	423	2.58

[a] $D_p = 0.9\lambda/\beta_{1/2}\cos\theta$; λ: X-ray source wavelength; $\beta_{1/2}$: full width half maximum; θ: angle.
[b] Band-gap values calculated by plotting photon energy (eV) versus square of absorption co-efficient $(\alpha h\nu)^2$.
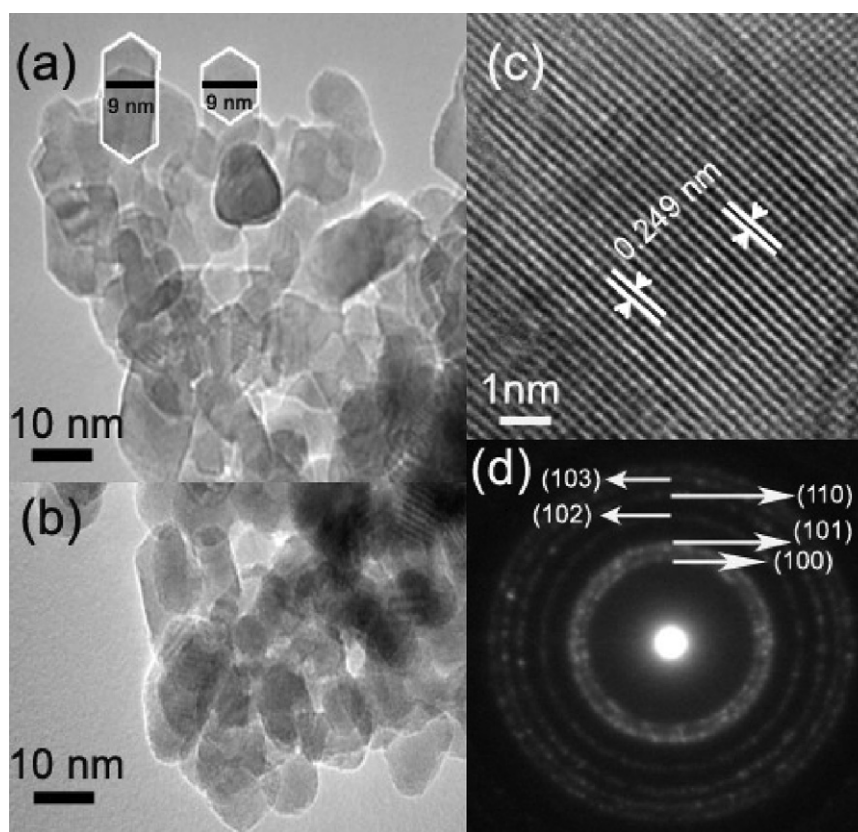
Fig. 2. (a), (b) TEM images, (c) HR-TEM image, and (d) selective electron diffraction pattern for $Cd_{0.1}Zn_{0.9}O$.

3.3. UV–vis spectroscopic analysis

The optical properties of $Cd_xZn_{1-x}O$ solid solutions, as measured by diffuse reflection spectrophotometer at room temperature, are displayed in Fig. 3. $Cd_xZn_{1-x}O$ solid solutions (Fig. 3a) showed intense absorption bands with steep edges in the visible-light region, being different from ZnO that has a UV absorption band. The shape of the spectrum indicates that the origin of visible-light absorption is not due to impurity levels in ZnO as observed for the other metal (Co^{2+}, Mn^{2+} and Ni^{2+}) doped ZnO [29,30]. The UV–vis absorption spectra of Cu^{2+}-modified photocatalysts were shown in Fig. 3b. When the Cu^{2+} ions were modified onto the pure ZnO, two additional absorption bands appeared in addition to the inter-band transition of ZnO (Fig. 3b). The small absorption ranging from 400–500 nm corresponds to interfacial charge transfer (IFCT) [7,25] and the strong absorption at $\sim$700–800 nm belongs to d–d transition of Cu^{2+} ions. However, in Cu^{2+}–$Cd_xZn_{1-x}O$, IFCT absorption was masked due to the strong visible-light absorption of $Cd_xZn_{1-x}O$ itself, though d–d transition is very clear similar like Cu–ZnO photocatalysts (Fig. 3b). Irie et al. reported the IFCT phenomenon in TiO_2 system, in which visible-light irradiation causes the interfacial electron transfer from the VB of TiO_2 to Cu^{2+} ions on the surface of TiO_2 photocatalysts.

UV–vis spectra of other metal (Co^{2+}, Mn^{2+} and Ni^{2+}) doped ZnO showed broad absorption peaks around 500–700 nm, in addition to band to band transition. These peaks at higher wavelength correspond to the formation of mid-gap state between the band-gap by the respective metal ions, which act as recombination centres and reduced the photocatalytic activity. Unlike other metal doped ZnO photocatalysts, in the present study, $Cd_xZn_{1-x}O$ photocatalysts did not absorb photon with longer wavelengths more than 550 nm, which hint that unoccupied defect levels were unlikely created in the band-gap of ZnO. The first principle study of CB structure $Cd_xZn_{1-x}O$ solid solutions revealed that the bottom of the CB (Zn 4s) gradually changed to Cd 5s, when the concentration of Cd increased [31]. It was also reported from the first principle study of $Cd_xZn_{1-x}O$, the VB position referring to vacuum level did not change during the incorporation of Cd into ZnO [32], therefore, the red-shift in the absorption edge was supposed to occur mainly due to the formation of Cd 5s levels near the CB edge of ZnO. The band structure of $Cd_xZn_{1-x}O$ photocatalysts were discussed in detail in the later section. Band-gap value of $Cd_xZn_{1-x}O$ photocatalysts were calculated by plotting photon energy (eV) versus square of absorption co-efficient $(\alpha h\nu)^2$, and the extrapolation of the linear portion of the graph to the energy axis gives the band-gap energy values (Fig. 3c). For pure ZnO, we obtained an E_g value of 3.13 eV, which is fairly concordance with the previously reported values [33]. The band-gap of the $Cd_xZn_{1-x}O$ (Table 1) was smaller than that of ZnO and decreased with the increasing concentration of cadmium. The band-gap was calculated to be 2.96, 2.81, 2.64, and 2.58 eV correspond to the different x (Cd) values of 0.05, 0.1, 0.20 and 0.25 (Fig. 3c).

The red-shift in the optical absorption of $Cd_xZn_{1-x}O$ can also be explained in terms of the ionic bond strength between metal ions and oxygen ions [34]. The electro-negativity values of Mg, Zn, Cd, and O are 1.3, 1.6, 1.7, and 3.4 respectively. The percentage of ionic character for Mg–O, Zn–O and Cd–O is 66.8, 55.5 and 51.5% respectively. Thus, the order of ionic nature is MgO > ZnO > CdO. Hence, the difference in energy levels between cation's s state, main component of the CB, and the O 2p are small in CdO, large in ZnO and largest in MgO. Therefore, the Mg doping into ZnO causes band-gap widening, while the Cd doping causes band-gap narrowing [35,36]. These results indicate that the band-gap reduction of ZnO was mainly due to the formation of Cd 5s state below the CB edge, which extend the absorption of ZnO into visible region.
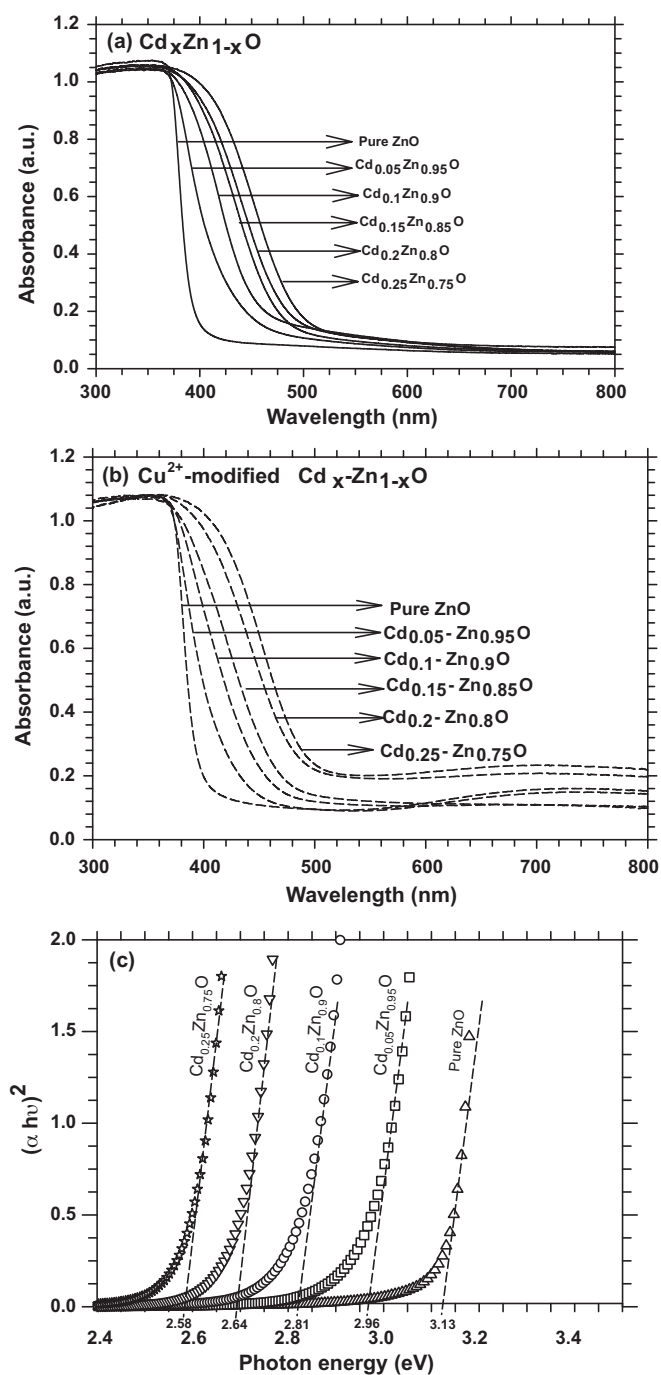
Fig. 3. UV–vis spectra of (a) ZnO and $Cd_xZn_{1-x}O$ photocatalysts; (b) Cu^{2+}-modified $Cd_xZn_{1-x}O$ photocatalysts; (c) band-gap calculation diagram for ZnO and $Cd_xZn_{1-x}O$ photocatalysts.

3.4. Photocatalytic studies

The photocatalytic activity of the ZnO, $Cd_xZn_{1-x}O$, and Cu^{2+}-modified $Cd_xZn_{1-x}O$ photocatalysts were evaluated by measuring the initial generation rate of carbon dioxide (CO_2). The results are shown in Fig. 4 and Table 3. Pure ZnO photocatalysts showed negligible visible-light photocatalytic activity (Table 3 and Fig. 4a), which is due to the large band-gap of ZnO and the lack of absorption in the visible region. In contrast, the $Cd_xZn_{1-x}O$ samples exhibited higher photocatalytic activities than pure ZnO photocatalyst as shown in Table 3 and Fig. 4a. The reaction rate (RR) of CO_2 increase with increasing loading of Cd with the maximum RR at $x = 0.10$
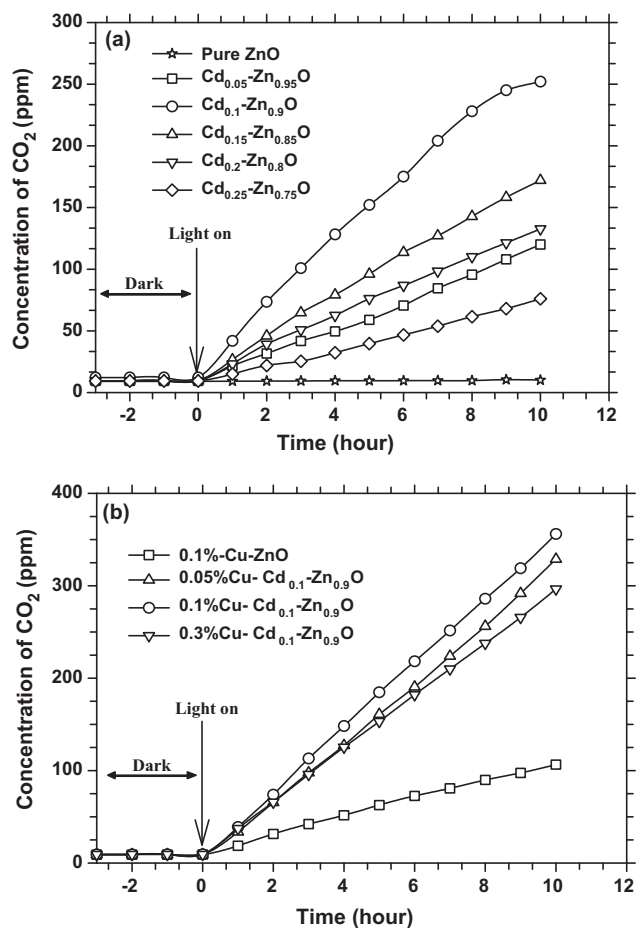

Fig. 4. Initial reaction rate of CO_2 over (a) $Cd_xZn_{1-x}O$ photocatalysts and (b) Cu^{2+}-modified $Cd_xZn_{1-x}O$ photocatalysts.

and further loading ($x = 0.15$, 0.2 & 0.25) resulted in the decrease of RR. Since the incorporation of Cd ions into ZnO photocatalyst decreases the reduction potential of electrons or causes lattice distortion of ZnO, the photocatalytic activity has to be reduced by too much addition of cadmium. The optimum amount of Cd (x) is 0.1, and the reaction rate of corresponding $Cd_{0.1}Zn_{0.9}O$ photocata-

Table 3
Dependance of photocatalytic activities for gaseous acetaldehyde decomposition under visible-light irradiation over $Cd_xZn_{1-x}O$ solid solutions upon the composition of Cd^{2+} and Cu^{2+}[a].

Material	Reaction rate of $CO_2(\times 10^{-10}$ mol/s)
Pure-ZnO	N. D.
Deg. P25	N. D.
$Cd_{0.05}Zn_{0.95}O$	0.94
$Cd_{0.1}Zn_{0.9}O$	1.54
$Cd_{0.15}Zn_{0.85}O$	1.34
$Cd_{0.2}Zn_{0.8}O$	1.0
$Cd_{0.25}Zn_{0.75}O$	0.89
0.05% Cu^{2+}–$Cd_{0.1}Zn_{0.9}O$	1.94
0.1% Cu^{2+}–$Cd_{0.1}Zn_{0.9}O$	2.05
0.3% Cu^{2+}–$Cd_{0.1}Zn_{0.9}O$	2.05
0.1% Cu^{2+}–ZnO	0.58
0.1% Cu^{2+}–$Cd_{0.05}Zn_{0.95}O$	1.16
0.1% Cu^{2+}–$Cd_{0.1}Zn_{0.9}O$	2.05
0.1% Cu^{2+}–$Cd_{0.15}Zn_{0.85}O$	1.96
0.1% Cu^{2+}–$Cd_{0.2}Zn_{0.8}O$	1.04
0.1% Cu^{2+}–$Cd_{0.25}Zn_{0.75}O$	0.94

[a] Catalyst: 0.1 g, heat treated under black light for 3 h. Acetaldehyde: concentration 500 ppm. Light source: Blue LED ($\lambda = 400$–550 nm) without filter. Light intensity: 20 mW/cm².

lyst was 1.54×10^{-10} mol/s. The enhanced photocatalytic activity of $Cd_{0.1}Zn_{0.9}O$ under visible-light illumination attributed to the red-shift of adsorption edge of ZnO. The present photocatalytic evaluation was performed under the light-limited condition, not under the light-rich condition [37]. Therefore, the visible-light activity in the present study strongly depends on the electron-hole charge separation efficiency, even if the $Cd_xZn_{1-x}O$ has larger surface area than pure ZnO. We have optimized the several experimental conditions by varying the (i) hydrothermal reaction time and (ii) hydrothermal reaction temeprature, and (iii) the effect of annealing temperature in order to achieve the high photocatalytic activity of $Cd_xZn_{1-x}O$ solid solutions. The results and discussion were included in our supporting information (ESI†, Figs. S3 and S4).

Further enhancement in the photocatalytic activity of optimized $Cd_xZn_{1-x}O$ photocatalysts was observed over Cu^{2+} modification as shown in Fig. 4b. The Cu^{2+} modified ZnO exhibited visible-light photocatalytic activity because of IFCT [7]. However, the IFCT is surface phenomenon [38,39], and hence the aborption by IFCT is slight. Therefore, the visible-light activity by IFCT is relatively low. On the other hand, when the Cu^{2+} ions were modified onto the surface of $Cd_xZn_{1-x}O$ solid solutions, their photocatalytic activity was greatly enhanced. Irie et al. [7] previously investigated the role of Cu(II) co-catalyst by X-ray absorption fine structure (XAFS) analysis. In situ XAFS measurements were performed under visible-light in the presence of 2-propanol and absence of oxygen. Under these conditions, Cu(I) was generated. However, the latter converted back to Cu(II) when it was exposed to oxygen, indicating the oxygen reduction activity of Cu(I). These results clearly indicate that the electrons in Cu(I) ions can cause the reduction reaction of absorbed oxygen molecules. We suppose that the produced Cu(I) reduces O_2 through a multi-electron reduction process. Several groups also reported that the possibilities of multi-electron reductions in Cu ions [40–43]. Very importantly, the Cu(II) ions were not changed in air condition, even after the photocatalytic oxidative reaction, and the turnover numbers of this reaction is more than 4. It means the Cu(II) ion is very stable co-catalyst to cause multi-electron reduction. In order to optimize the amount of Cu^{2+} over $Cd_xZn_{1-x}O$, a series of photocatalytic experiments for the decomposition of acetaldehyde with varied Cu^{2+} concentrations (0.05%, 0.1%, and 0.3% Cu) carried out. Consequently, 0.1 wt.% of Cu^{2+} exhibited highest RR (2.0536×10^{-10} mol/s) and found as an optimum Cu^{2+} concentration for $Cd_xZn_{1-x}O$ solid solutions (Fig. 4b). With the optimized Cu^{2+} concentration, the photocatalytic experiments for the decomposition of acealdehyde done with varying Cd concentration ranging from $x = 0.05–0.25$ and the results are shown in Fig. S3d. These results conclude that Cu^{2+}-modified $Cd_xZn_{1-x}O$ ($x = 0.1$) exhibited the highest reaction rate among the samples. It is interesting to note that RR of Cu^{2+}-modified $Cd_xZn_{1-x}O$ is 1.5 times higher than that of $Cd_xZn_{1-x}O$ without Cu^{2+} modification. This is quite reasonable due to the fact that the visible-light-excited electrons in $Cd_xZn_{1-x}O$ are transferred to Cu^{2+} ions and they can react with oxygen molecules through multi-electron reduction reaction. Hence, the recombination of holes and electrons is retarded in this system. The reaction rate of optimized photocatalyst, 0.1% $Cu^{2+}–Cd_{0.1}Zn_{0.9}O$ was 3.5 and 1.5 times higher than $Cu^{2+}–ZnO$ and $Cd_{0.1}Zn_{0.9}O$ photocatalysts respectively.

Initial concentration of acetaldehyde was 500 ppm, thus generated CO_2 should be reached to 1000 ppm for the complete decomposition. The results of complete decomposition of acetaldehyde for optimized samples (0.1% $Cu^{2+}–ZnO$, $Cd_{0.1}Zn_{0.9}O$, 0.1% $Cu^{2+}–Cd_{0.1}Zn_{0.9}O$) are shown in Fig. 5. Cu^{2+}-modified ZnO exhibited visible-light activity better than pure ZnO, owing to the visible-light absorption by IFCT [7]. However, these $Cu^{2+}–ZnO$ could not completely decompose acetaldehyde under visible-light irradiation for 100 h. In contrast, $Cd_{0.1}Zn_{0.9}O$ could completely decompose acetaldehyde, further, the Cu^{2+}-modification greatly
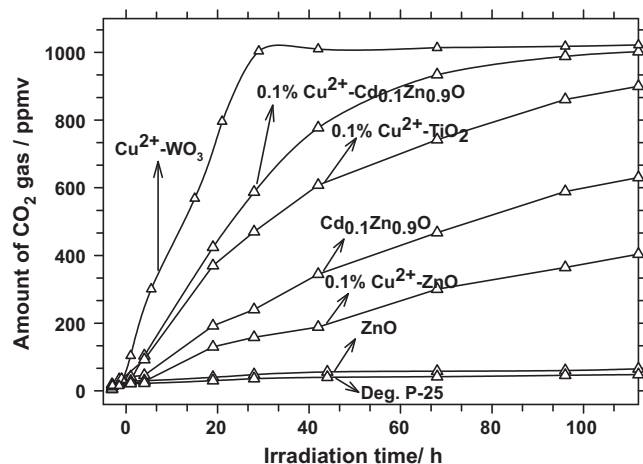

Fig. 5. Changes in CO_2 concentrations due to the decomposition of acetaldehyde as a function of time under visible-light at 400–550 nm (light intensity: 20 mW/cm²).
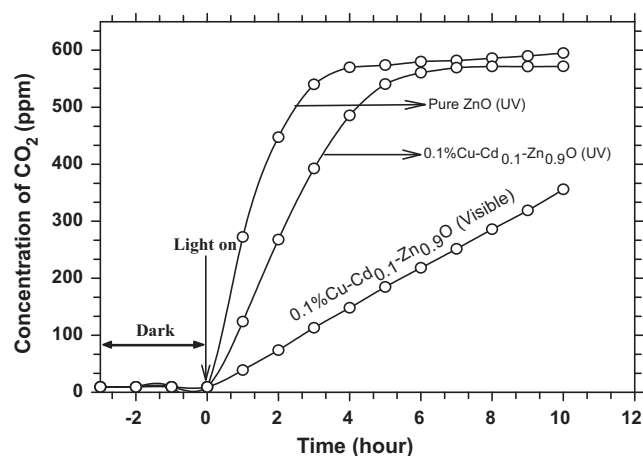

Fig. 6. Comparison of photocatalytic activity of ZnO and 0.1%$Cu^{2+}–Cd_{0.1}Zn_{0.9}O$ photocatalysts under UV and visible-light illumination with similar absorbed photon numbers (8.5×10^{15} quanta/cm²/s).

enhanced its visible-light activity. After visible-light irradiation for ca 70 h, nearly 1000 ppm of CO_2 was generated, indicating a complete oxidation of acetaldehyde into CO_2 over 0.1% Cu^{2+}-modified $Cd_{0.1}Zn_{0.9}O$. Whereas, under the same irradiation time only 630 ppm and 404 ppm of CO_2 generated for $Cd_{0.1}Zn_{0.9}O$ and $Cu^{2+}–ZnO$ respectively. This indicates that neither the band engineering by CB control nor the multi-electron reduction by surface modification alone can produce the highly efficient visible-light active photocatalyst. We compared our 0.1% $Cu^{2+}–Cd_{0.1}Zn_{0.9}O$ with a Cu^{2+}-TiO_2 and $Cu^{2+}–WO_3$ photocatalysts prepared by the same procedure [7] and TiO_2 (Degussa P-25), a well known photocatalyst. The visible-light photocatalytic activity of our photocatalyst, 0.1% Cu^{2+}-modified $Cd_{0.1}Zn_{0.9}O$ was better than Cu^{2+}-modified TiO_2 and P-25 and less than $Cu^{2+}–WO_3$ as shown in Fig. 5. P-25 showed negligible visible-light photocatalytic activity. Although, the photocatalytic activity of 0.1% $Cu^{2+}–Cd_{0.1}Zn_{0.9}O$ was less than that of $Cu^{2+}–WO_3$, the former ZnO-based visible-light photocatalysts have several advantages such as in-expensive, easily available and stable as compared to WO_3 photocatalysts.

The UV and visible-light photocatalytic activities of 0.1% Cu^{2+}-modified $Cd_{0.1}Zn_{0.9}O$ are shown in Fig. 6 in order to discuss its electronic band structure. The UV-light experiment of 0.1% Cu^{2+}-modified $Cd_{0.1}Zn_{0.9}O$ carried out under the same absorbed photons conditions as used in visible-light experiment by controlling their light intensities (calculation method for absorbed photon numbers

and light spectra of UV & visible region were shown in our supporting information, Fig. S5). The reaction rate of 0.1% Cu^{2+}-modified $Cd_{0.1}Zn_{0.9}O$ under visible-light was five times less than that under UV light illumination, although the number of absorbed photons (8.5×10^{15} quanta/cm^2/s) was identical regardless of the illumination source. If the Cd 5s levels mixed with the Zn 4s orbital (CB edge of ZnO) and the band-gap narrowed, then the photo-generated electrons in the CB would diffuse to the lower edge of the CB by a radiative process. Under these conditions, the photocatalytic activity should be identical for both UV and visible-light illumination with the same absorbed photon numbers. However, the experimental results revealed that the quantum yield (QY) of 0.1% Cu^{2+}-modified $Cd_{0.1}Zn_{0.9}O$ under visible-light was less than that under UV light. These results suggest that Cd 5s levels supposed to form a shallow state below the CB rather than shifting the CB positively. The shallow states below the CB edge localized the electrons and decrease the mobility of electrons, which decrease the photocatalytic activity under visible-light. Hence it is confirmed that Cd 5s levels formed a shallow states below the CB edge, even though UV–vis absorption spectra of $Cd_{0.1}Zn_{0.9}O$ solid solution seems to narrow its band-gap by forming continuous band structure with the bottom of the CB edge. In case of nitrogen doped TiO_2, QY under visible-light was 37 times less than that under UV light [4]. Low QY of nitrogen doped TiO_2 under visible-light is due to the formation of isolated band of N 2p orbital above the VB. In contrast to the nitrogen doped TiO_2, the QY of 0.1% Cu^{2+}-modified $Cd_{0.1}Zn_{0.9}O$ under visible-light was not so deteriorated versus that under UV light irradiation (only 5 times less than UV light). In case of N-doped TiO_2, as reported earlier, the isolated levels of the N 2p orbital placed above the VB, and thus, holes produced by visible-light illumination are localized and have a slower mobility. Whereas in the present system, 0.1% Cu^{2+}-modified $Cd_{0.1}Zn_{0.9}O$ photocatalysts, the levels of Cd 5s are shallow states below the CB edge, then the electron hopping process is expected and their mobility should be larger than those of holes in the isolated levels of N 2p orbital. Further, the addition of co-catalysts (Cu^{2+}), paves the way for the efficient electron extraction from the shallow states below the CB edge, keeping the VB level deep enough to cause the strong oxidation activity. Therefore, the strong oxidative power of holes and the effective charge separation are achieved in our 0.1% Cu^{2+}-modified $Cd_{0.1}Zn_{0.9}O$ system. We also evaluated the UV light activity for pure ZnO under the same absorbed photon numbers with those of Cu^{2+}-modified $Cd_{0.1}Zn_{0.9}O$ (Fig. 6). Although the UV light activity of Cu^{2+}-modified $Cd_{0.1}Zn_{0.9}O$ was less than that of pure ZnO, its activity was not so deteriorated as compared to the nitrogen doped TiO_2 system, indicating the mobility of photo-generated electrons in $Cd_{0.1}Zn_{0.9}O$ was not largely decreased. In general, QY of a metal-ion-doped semiconductor [1] is much less than that of un-doped semiconductor. The deep impurity levels produced in the forbidden band of the photocatalysts by the metal ion, act as recombination centres, and accounting for the low-photocatalytic activity. However, in the present study, Cd 5s states in $Cd_{0.1}Zn_{0.9}O$ are shallow, and the efficient visible-light-active photocatalyst can be developed with keeping the high QY under UV light.

3.5. Stability studies

The stability of $Cd_xZn_{1-x}O$ photocatalysts was tested by dispersing 0.1 g photocatalysts in 50 mL water followed by exposure of visible-light/dark conditions. The details of stability test experiment and radio-frequency inductive coupled plasma (rf-ICP) analysis were mentioned in the experimental section. rf-ICP analysis revealed that Cd^{2+} and Zn^{2+} ions in $Cd_xZn_{1-x}O$ photocatalysts were not dissolved in water during the exposure of visible-light as well in dark for one day. In order to check the long-term stability of photocatalysts, the reaction had been carried out for long time
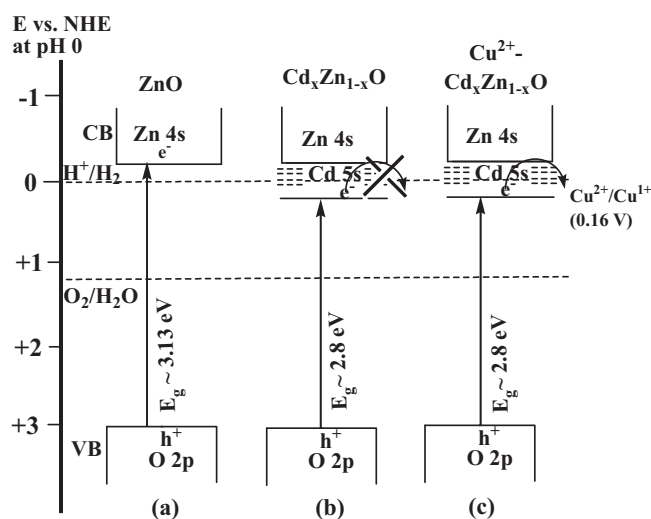

Fig. 7. Schematic illustration of band structures of ZnO (left), $Cd_xZn_{1-x}O$ (centre) and Cu–$Cd_xZn_{1-x}O$ (right).

(one week) by the continuous exposure of visible-light as well as in dark. The rf-ICP analysis of the resulting samples reveals that there was no Cd and Zn dissolution from $Cd_xZn_{1-x}O$ photocatalysts. The present results indicate that $Cd_xZn_{1-x}O$ act as a stable visible-light-driven photocatalyst under visible-light illumination at neutral conditions.

3.6. Band structure

Based on the characterization and photocatalytic activities we speculate the band structures for bare ZnO, $Cd_xZn_{1-x}O$ and Cu^{2+}-modified $Cd_xZn_{1-x}O$ as shown in Fig. 7. In Fig. 7a, O 2p orbitals contribute to making up a VB while Zn 4s contribute to a CB. Since the distance between the VB (O 2p) and the CB (Zn 4s) of pure ZnO was large (3.31 eV) (Fig. 7a), it can not absorb visible-light. Hence, ZnO showed negligible photocatalytic activity for the decomposition of acetaldehyde. On the other hand, $Cd_xZn_{1-x}O$ solid solutions (Fig. 7b), Cd 5s orbitals mixed with Zn 4s contribute to forming a CB, and the CB minimum composed of hybrid orbitals Zn 4s + Cd 5s, which can be shift the CB positively. The proposed band structures of $Cd_xZn_{1-x}O$ solid solutions are consistent with UV–vis absorption spectra of $Cd_xZn_{1-x}O$ photocatalysts. However, the UV light photocatalytic activity results indicated that Cd 5s levels are forming shallow state rather than continuous levels with the CB edge of ZnO (Fig. 7b). It is also interesting to note that the VB position of $Cd_xZn_{1-x}O$ is enough deep as pure ZnO, thus the oxidation power of photogenerated holes will be enough high to decompose organic compounds. Even though the $Cd_xZn_{1-x}O$ has the ability to absorb visible-light and increase the photocatalytic activity, mobility and reduction potential of electrons in un-continuous Cd 5s levels seems to be lower than that in CB of pure ZnO. Hence, in the present study, Cu^{2+} cocatalysts were modified onto $Cd_xZn_{1-x}O$ (Fig. 7c) to increase the reduction ability of electrons by an efficient multi-electron reduction process. Therefore, holes with strong oxidation power are generated in VB of $Cd_xZn_{1-x}O$, and electrons in CB are effectively separated into the high reductive sites of Cu^{2+} ions upon visible-light irradiation.

4. Conclusion

In summary, we have designed an efficient ZnO-based visible-light driven photocatalyst based on band-gap engineering ($Cd_xZn_{1-x}O$) and surface modification (Cu^{2+}). Characterization and

photocatalytic results show Cd^{2+} incorporated into ZnO formed an shallow state below the conduction band and effectively extend the absorption edge into the visible region. In addition, the strong oxidative power and high mobility of holes produced in the valence band upon visible-light illumination. $Cd_xZn_{1-x}O$ showed high photocatalytic activities under visible-light illumination as compared to pure ZnO. Further, Cu^{2+} modification ensure the enhancement in the visible-light activity of $Cd_xZn_{1-x}O$ by capturing the photo-excited electrons. Comparison of the quantum yields between UV and visible-light illuminations reveals the present system (Cu^{2+}-modified $Cd_xZn_{1-x}O$) has higher oxidation power and mobility of holes than N-doped TiO_2. The high-sensitive rf-ICP analysis confirms that the designed photocatalyst was stable in water under visible-light irradiation. The hybrid approach developed here for the first time in ZnO photocatalysts, will be very useful to fabricate visible-light photocatalyst using various low-cost, and wide band-gap semiconductors.

Acknowledgements

Appendix A. Supplementary data

Supplementary data associated with this article can be found, in the online version, at doi:10.1016/j.apcatb.2010.08.029.

References

[1] J.G. Highfield, P. Pichat, New. J. Chem. 13 (1989) 61–66.
[2] R. Asahi, T. Morikawa, T. Ohwaki, K. Aoki, Y. Taga, Science 293 (2001) 269–271.
[3] H. Irie, Y. Watanabe, K. Hashimoto, J. Phys. Chem. B 107 (2003) 5483–5486.
[4] M. Miyauchi, A. Ikezawa, H. Tobimatsu, H. Irie, K. Hashimoto, Phys. Chem. Chem. Phys. 6 (2004) 865–870.
[5] R. Nakamura, T. Tanaka, Y. Nakato, J. Phys. Chem. B 108 (2004) 10617–10620.
[6] R. Abe, H. Takami, N. Murakami, B. Ohtani, J. Am. Chem. Soc. 130 (2008) 7780–7781.
[7] H. Irie, S. Miura, K. Kamiya, K. Hashimoto, Chem. Phys. Lett. 457 (2008) 202–205.
[8] T. Arai, M. Horiguchi, M. Yanagida, T. Gunji, H. Sugihara, K. Sayama, Chem. Commun. (2008) 5565–5567.
[9] Y.H. Kim, H. Irie, K. Hashimoto, Appl. Phys. Lett. 92 (2008) 182107.
[10] T. Torimoto, N. Nakamura, S. Ikeda, B. Ohtani, Phys. Chem. Chem. Phys. 4 (2002) 5910–5914.
[11] H.G. Yu, H. Irie, K. Hashimoto, J. Am. Chem. Soc. 132 (2010) 6898–6899.
[12] Z.L. Wang, ACS Nano. 2 (2008) 1987–1992.
[13] M. Law, L.E. Greene, J.C. Johnson, R. Saykally, P.D. Yang, Nat. Mater. 4 (2005) 455–459.
[14] M.H. Huang, S. Mao, H. Feick, H.Q. Yan, Y.Y. Wu, H. Kind, E. Weber, R. Russo, P.D. Yang, Science 292 (2001) 1897–1899.
[15] A. Tsukazaki, A. Ohtomo, T. Onuma, M. Ohtani, T. Makino, M. Sumiya, K. Ohtani, S.F. Chichibu, S. Fuke, Y. Segawa, H. Ohno, H. Koinuma, M. Kawasaki, Nat. Mater. 4 (2005) 42–46.
[16] J. Goldberger, D.J. Sirbuly, M. Law, P.D. Yang, J. Phys. Chem. B 109 (2005) 9–14.
[17] H. Kind, H.Q. Yan, B. Messer, M. Law, P.D. Yang, Adv. Mater. 14 (2002) 158–160.
[18] Q. Wan, Q.H. Li, Y.J. Chen, T.H. Wang, X.L. He, J.P. Li, C.L. Lin, Appl. Phys. Lett. 84 (2004) 3654.
[19] Z.L. Wang, J.H. Song, Science 312 (2006) 242–246.
[20] S. Sakthivel, B. Neppolian, M.V. Shankar, B. Arabindoo, M. Palanichamy, V. Murugesan, Sol. Energy Mater. Sol. Cells 77 (2003) 65–82.
[21] K. Maeda, T. Takata, M. Hara, N. Saito, Y. Inoue, H. Kobayashi, K. Domen, J. Am. Chem. Soc. 127 (2005) 8286–8287.
[22] X. Qiu, G. Li, X. Sun, L. Li, X. Fu, Nanotechnology 19 (2008) 215703.
[23] R.A. Vanleeuwen, C.J. Hung, D.R. Kammler, J.A. Switzer, J. Phys. Chem. 99 (1995) 15247–15252.
[24] R.D. Shannon, Acta Crystallogr. A 32 (1976) 751–767.
[25] H. Irie, K. Kamiya, T. Shibanuma, S. Miura, D.A. Tryk, T. Yokoyama, K. Hashimoto, J. Phys. Chem. C 113 (2009) 10761–10766.
[26] F. Wang, B. Liu, C. Zhao, S. Yuan, Mater. Lett. 63 (2009) 1357–1359.
[27] C. Calareso, V. Grasso, L. Silipigni, Appl. Surf. Sci. 171 (2001) 306–313.
[28] S.W. Gaarenstroom, N. Winograd, J. Chem. Phys. 67 (1977) 3500–3506.
[29] Q. Xiao, J. Zhang, C. Xiao, X. Tan, Mater. Sci. Eng. B 142 (2007) 121–125.
[30] S. Ekambaram, Y. Iikubo, A. Kudo, J. Alloys Compd. 433 (2007) 237–240.
[31] Z.J. Wang, I. Tanaka, Mater. Trans. 50 (2009) 1067–1070.
[32] X.D. Zhang, M.L. Guo, W.X. Li, C.L. Liu, J. Appl. Phys. 103 (2008) 063721.
[33] H. Cao, J.Y. Xu, D.Z. Zhang, S.H. Chang, S.T. Ho, E.W. Seeling, X. Liu, R.P.H. Chang, Phys. Rev. Lett. 84 (2000) 5584–5587.
[34] B. Viswanathan, Bull. Catal. Soc. India 2 (2003) 71–74.
[35] M.K. Yadav, M. Ghosh, R. Biswas, A.K. Raychaudhuri, A. Mookerjee, S. Data, Phys. Rev. B 76 (2007) 195450.
[36] H.C. Hsu, C.Y. Wu, H.M. Cheng, W.F. Hsieh, Appl. Phys. Lett. 89 (2006) 013101.
[37] Y. Ohko, K. Hashimoto, A. Fujishima, J. Phys. Chem. A 101 (1997) 8057–8062.
[38] C. Creutz, B.S. Brunschwig, N. Suntin, J. Phys. Chem. B 109 (2005) 10251–10260.
[39] C. Creutz, B.S. Brunschwig, N. Suntin, J. Phys. Chem. B 110 (2006) 25181–25190.
[40] F. Himo, L.A. Eriksson, F. Maseras, P.E.M. Siegbahn, J. Am. Chem. Soc. 122 (2000) 8031–8036.
[41] S. Goldstein, G. Czapski, R. Van Eldik, H. Cohen, D. Meyerstein, J. Phys. Chem. 95 (1991) 1282–1285.
[42] N. Kitajima, Y. Moro-oka, Chem. Rev. 94 (1994) 737–757.
[43] A.P. Cole, D.E. Root, P. Mukherjee, E.I. Solomon, T.D.P. Stack, Science 273 (1996) 1848–1850.